Nanoscale

Accepted Manuscript

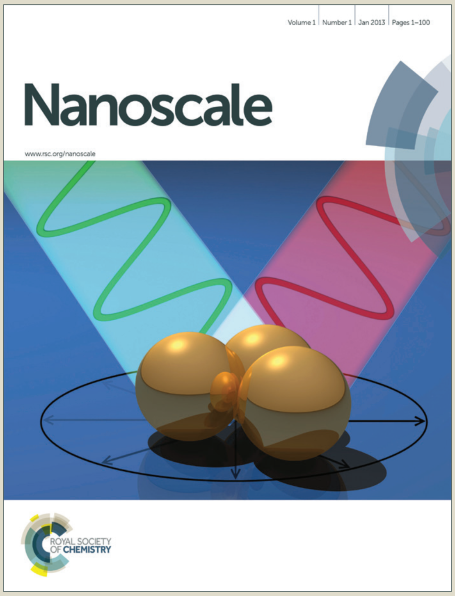

ROYAL SOCIETY OF CHEMISTRY

www.rsc.org/nanoscale

Cite this: DOI: 10.1039/c0xx00000x

www.rsc.org/xxxxxx

ARTICLE TYPE

Vacancy Interlayer Migration in Multi-layered Graphene

Lili Liu,[a] Junfeng Gao,[b] Xiuyun Zhang,[b] Tianying Yan[c] and Feng Ding[a,b*]

Received (in XXX, XXX) Xth XXXXXXXXX 20XX, Accepted Xth XXXXXXXXX 20XX
DOI: 10.1039/b000000x

The migration of vacancies between graphene layers or carbon nanotube walls was broadly observed in experiments, wherein, it was well known that the migration of vacancies between adjacent layers is prohibited by a very large barrier (~ 7.0 eV). The contradiction leads to a big puzzle for many years. In this study, by using density functional tight-binding molecular dynamic simulations and first principle calculations, we found that interaction between vacancies or vacancy holes in neighboring graphene layers can greatly reduce the barrier to ~ 3 eV or less and expedites the migration process. And all the vacancies in a multi-layered graphene gather to form a single hole in one layer. Our study revealed a new mechanism of the defect healing in grahene materials and successfully explained the experimental puzzle. Our results may have important applications in engineering desired graphene materials.

Introduction

Graphene has innumerous applications, such as electronics, energy generation and conversion and composite materials, due to its exceptional electronic, thermal, mechanical and chemical properties.[1-3] Various defects that can be introduced into the graphene lattice during synthesis and/or post-treatments [4] are known have significantly impact on these properties. [5-9] So engineering graphene by introducing or annihilating defects is an important technology to achieve desired properties for various applications. Therefore a comprehensive understanding on the behavior of defects in graphene is critically important. In previous studies, vacancy formation and migration in single layer graphene (SLG) or single walled carbon nanotubes (SWCNTs) has been extensively studied. [10-14] It is found that single vacancy (SV) is highly mobile while multi-fold ones are normally very stable.[14-16] Experimentally, vacancies in graphene and CNTs are broadly introduced by electron or iron radiation. With the assistance of the high resolution transmission electron microscopy (TEM) or scanning tunneling microscopy (STM), their formation process and migration behavior in MLG or multi-walled carbon nanotubes (MWCNTs) have been extensively explored. [9, 15, 18, 19] While the understanding on their behaviors, especially the interlayer interaction and migration, are very limited. Due to the highly anisotropic structure of MLG or MWCNT, it was normally assumed that a vacancy in MLG or MWCNT behaved very similar as that in SLG or SWCNT.
Especially, previous theoretical calculations have shown that the vacancy migration between layers is prohibited by the very high migration barrier (~7.0 eV).[20, 21] On the other hand, experimental observations normally showed that the irradiation of MLG or MWCNTs created vacancies in all graphene layers or MWCNT walls at the beginning, and further leaded to the formation of vacancy hole in one layer or wall only. [19, 22, 23] These observations imply that the vacancies created in various graphene layers can be gathered into one layer and thus the inter-layer migration of vacancies is unavoidable. While, the understanding on the vacancy migration between layers is still pending.

In present study, in order to achieve a full understanding on vacancy's interlayer migration, we systematically explored the kinetics of vacancy formation and the migration behavior in both SLG and MLG. It was found that, although the direct migration of a vacancy between neighboring graphene layers (NGLs) is prohibited, the interaction between vacancies or vacancy holes in NGLs can greatly reduce the migration barrier and speed up the vacancy migration process by 10-20 orders of magnitudes. Based on this study, the experimental puzzle mentioned above is well understood and a new mechanism of graphene self-healing is proposed.

Methods

The quantum mechanics molecular dynamics (QM/MD) simulations based on the density-functional tight-binding (DFTB) method, which is implemented in the DFTB+ software package, [24-27] was used to explore the vacancy migration in both SLG and MLG. Facilitated with a time step of 0.2 fs, the velocity Verlet algorithm is used for time integration. A Nose-Hoover thermostat with a reselecting probability of 0.2 is used to control the temperature. Both SLG and MLG were modeled with the periodic boundary condition (PBC) and the DFTB/MD simulations were performed at 2000K, 2500K and 3000K, respectively. The electronic temperature of 1000K was used in all the MD trajectories to allow an open-shell electronic structure to be effectively simulated in situations with near-degeneracy among the frontier orbitals. In addition, the Slater-Kirkwood dispersion is involved in the MD calculation. Ab initio calculations were

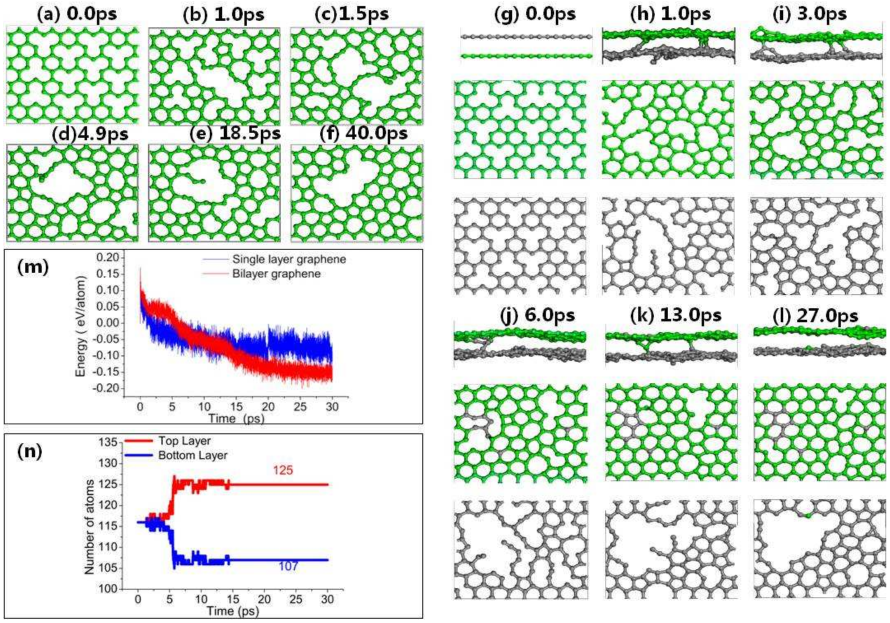

Fig. 1 The defect migration in graphene explored by molecular dynamic simulations (MD) at 2500 K. (a-f), snapshots of a MD trajectory of single layer graphene (SLG). (g-l), snapshots of a MD trajectory of bilayer graphene (BLG). (m) the relative energy as a function of time in both MD trajectories; (n), the number of carbon atoms in each layer of graphene vs. time in the MD trajectory of BLG.

performed by using density functional theory (DFT) and plane wave basis, as implemented in the Vienna Ab-initio Simulation Package (VASP).[28, 29] Generalized gradient approximation (GGA) with the Perdew-Burke-Ernzerhof (PBE) functional [30] was adopted to describe the exchange-correlation interaction, which was proved that it was elaborately developed for the calculations of surface systems. The core electrons were described by the projected augmented wave (PAW) method. [31] In addition, the plane wave basis set with an energy cutoff of 400 eV was used and the criterion of convergence was set as the force on each atom smaller than 0.03 eV/Å. Besides, all the transition states and barriers were calculated by the climbing nudged energy band (cNEB) [32] method and convergence criterion of 10-4 eV for total energy during the self-consistent field (SCF) calculations were used.

For the monolayer and bilayer MD simulation models, 116 C atoms for one layer within AB stacking and higer vacancy concentration with 12 vacancies randomly locating on the graphene due to the expensive calculations. A supercell (17.14 Å × 19.81 Å) were used for the model, and the layer distance is 3.4 Å, while the supercell dimension perpendicular to the graphene surface was chosen as large as 100 Å.

In addition, in the cNEB calculation models, during the geometry optimization, a (2 × 2 × 1) k-point mesh including the G point was used to sample the reciprocal space due to the large supercell. And the supercell (12.78 Å × 12.30 Å × 20.0 Å) is applied.

Results and discussion

We consider the evolution of vacancies in a SLG firstly. Typical snapshots of a DFTB/MD trajectory at 2500 K are shown in Fig. 1(a-f). In the initial configuration, 12 well dispersed SVs are created in each super cell of the graphene lattice (Fig. 1a). At the beginning of the simulation, the rebinding of dangling bonds of the densely distributed SVs results in the formation of pentagons, short C chains and small vacancy holes (Fig. 1b). Then these defects coalescent together to form larger holes and longer C chains (Fig. 1c). Finally, after a 40 ps MD simulation, only one large hole and a few topological defects are shown in

In order to find out the distinct vacancy evolution behavior in MLG, two SLGs with similar vacancy structures were placed together at a distance of 0.34 nm (Fig. 1g) and then MD trajectories were performed at exact same conditions. Exact same as that observed in the MD simulation of the SLG, holes, pentagons and short C chains were formed in both layers (Fig. 1g-i) in the first few ps. Besides the intra-layer evolution, the interlayer C-C binding could be seen from the beginning of the simulation (Fig. 1g-h). After a certain period of MD simulation, a distinct behavior—the interlayer C atom or vacancy migration was seen (see Fig. 1i-j). At the end of the trajectory, as a consequence of vacancy migration, only one large hole was formed in the bottom graphene layer and the top layer had only a few dangling bonds and topological defects. The atomic migration can be clearly seen in Fig. 1n. There were 116 atoms in each layer of the initial configuration and the numbers of atoms in the top and bottoms layers changed to be 125 and 107, respectively at the end of the trajectory. This implied a net mass migration of 9 atoms from bottom layer to the top one. Careful exam the final configuration reveals that there are actually 10 C atoms migrate upwards (from the bottom layer to the top one) and one C atoms moved downwards (Fig. 1i).

The observation of the interlayer vacancy migration in the MD simulation is surprising because the energy barrier of single vacancy migrate between two adjacent graphene layers is known as about 7.0 eV [21] (see Fig. 3a as well). Overcoming such a barrier at the temperature of 2500 K in so short a trajectory is nearly impossible. So, what is the undermined mechanism for the large number of vacancy migration in such a short period? What

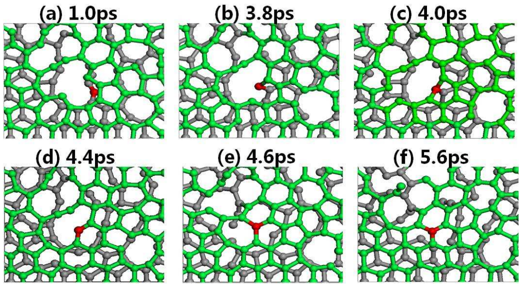

Fig. 2 Vacancy migration process between neighboring graphene layers as recorded in the MD simulation at 2500 K. Red color is used to highlight the carbon atom migrates from bottom layer to the top layer.

is the driving force that leads the atomic migration between neighboring layers?

Fig. 2 shows the details of a migration event. Firstly, an atom located at the edge of a hole in the bottom layer flipped up and contacted with a C atom on the edge of a hole in the top layer (Fig. 2a, b, c). Then the connection between the atom and the bottom layer broke, and another C-C bond on the top layer was formed (Fig. 2d-e). This new connection can reduce the energy of the system.[33] Eventually, further annealing eliminated the vacancy-hole in the top layer and sealed the migrated C atom into the lattice of top layer (Fig. 2f). From Fig. 2, one can see that the key of the atomic migration is the formation of the interlayer binding.

Fig. 3a presents the process of a single vacancy migration between two neighboring graphene layers (the vacancy in the top layer migrates towards the bottom layer by drawing one C atom from the bottom layer to healing the vacancy on the top layer and creating another vacancy in the bottom layer concurrently. The binding between one dangling atom of the vacancy in the top layer and another atom from the bottom layer forms the transition state). Because the interlayer binding has destroyed the perfect graphene lattice of the bottom layer, the transition state has very high formation energy (7.33 eV). So high a barrier implies that the direct migration of vacancies between grapnene layers is prohibited because such a single event would averagely costs $10^{-13} \times \exp(E^*/kT) \sim 10^3$ s of time at T = 2500 K. Certainly, the observation of any vacancy migration through such a mechanism in the time scale of 10 ps is impossible.

Although the direct migration of vacancy between graphene layers is prohibited, the migration can be facilitated by the interaction between two vacancies in neighboring layers. There are some bond unsaturated C atoms near each vacancy or vacancy hole in graphene and thus the temporary inter-layer connection between two bond unsaturated C atoms in NGLs should be much easier than that between two perfect graphene layers or a perfect one and one with a defect. As shown in Fig. 3b, two single vacancies were created in both layers, the contact of the two dangling bonds of each layer formed an stable intermediate structure which is 2.13 eV lower than the initial one. Then the migration of one C atom from one layer to the neighboring layer formed a low energy configuration in which the top layer was perfect and a pentagon-octagon-pentagon (5|8|5) divacancy (DV) was formed in another layer. Due to the fact that the formation energy of a DV is much lower than that of a SV, [34-36] a huge energy drop of 6.01 eV after migration is shown in Fig. 3b. Because of the great energy reduction of the final state, the energy barrier of such a migration process is 3.86 eV only, which is significantly lower than that of one SV migrating between neighboring graphene layers (Fig. 3a).

From above calculation, we can see that the inter-layer migration of vacancy or C atom can be facilitated by the interaction between defects in NGLs. Because the interlayer binding between two defects in NGLs can be easily built, the barrier of inter-layer vacancy/atom migration would be significantly decreased. To further confirm this idea, the migration of a SV to a graphene layer with a vacancy hole has been explored. As shown in Fig. 3c, the barrier of the vacancy migrating to a hole in the neighboring graphene layer is only 3.66 eV and a significant energy drop of 7.19 eV is shown. The great energy reduction is due to the build-up of perfect graphene lattice in the top layer. At the same time, all the single point energies of the DFT-obtained transition states in Fig.3 were calculated by DFTB method, which showed the same tendency. (The energy barriers are shown in the supporting information with Table 1).

Above calculations clearly indicates that the barrier of vacancy migration between graphene layers can be significantly decreased

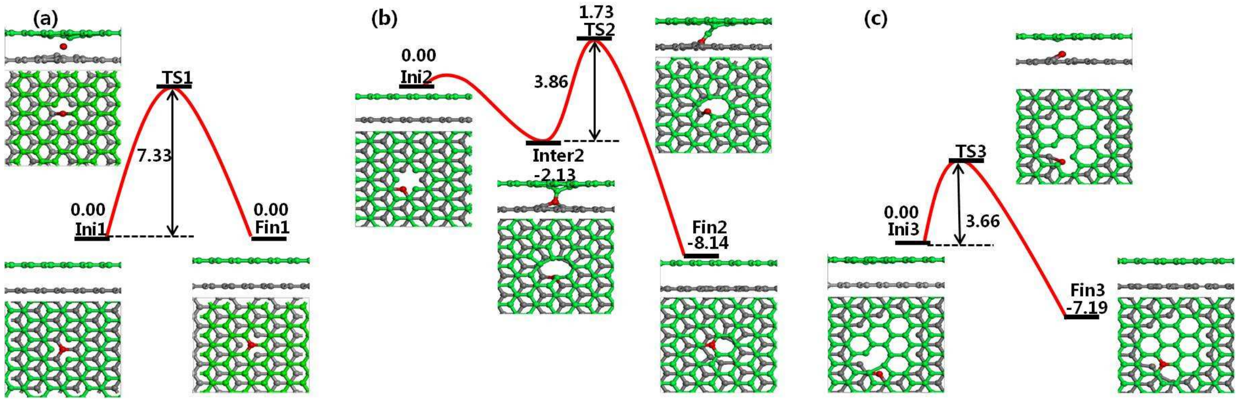

Fig. 3 (a) The transition state and barrier (in eV) of a single vacancy migrating between two neighboring graphene layers; (b) The migration process of a single vacancy from one graphene layer to a neighboring one which also has a vacancy in it; (c) The migration process of a single vacancy from the top graphene layer to another layer that has a hole (bottom layer). Red color is used to highlight the key atoms that diffused between graphene layers (All the optimized structures and their total energies we used are in supporting information)

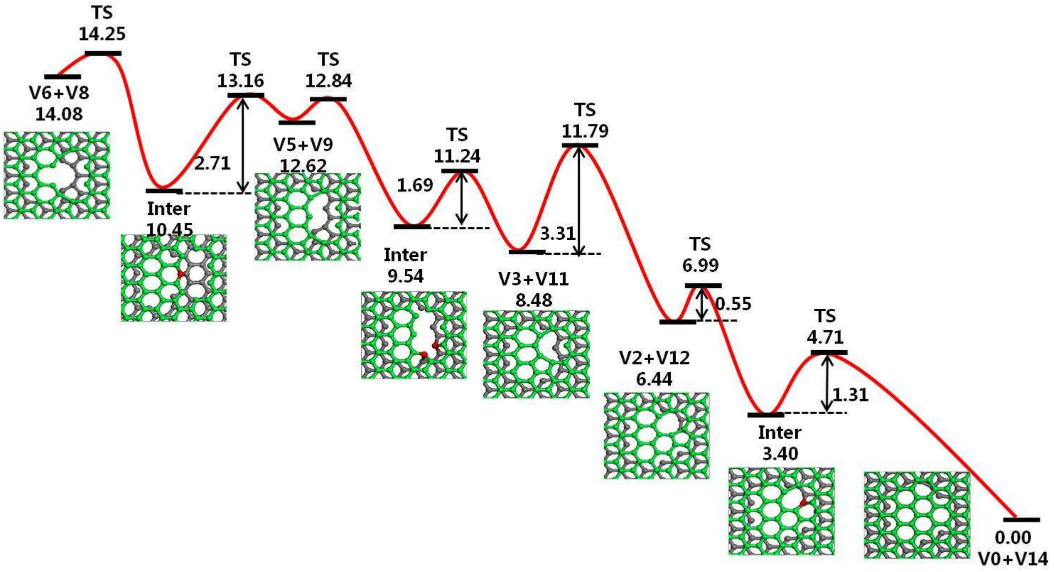

Fig. 4 (a) The transition state and barrier (in eV) of a single vacancy migrating between two neighboring graphene layers; (b) The migration process of a single vacancy from one graphene layer to a neighboring one which also has a vacancy in it; (c) The migration process of a single vacancy from the top graphene layer to another layer that has a hole (bottom layer). Red color is used to highlight the key atoms that diffused between graphene layers (All the optimized structures and their total energies we used are in supporting information).

by the interlayer interaction of the vacancies or other disorders and thus the migration of vacancies between graphene layers at a high temperature or facilitated by the electron irradiation is possible. Such a great barrier reduction facilitates the migration process by a factor of exp($\Delta E/kT$) ~ $10^{10} – 10^{20}$ at the temperature range of 1000 – 2500 K, where ΔE is the reduction of the energy barrier. To further understand the driving force of the interlayer migration of vacancies, let’s estimate the formation energy of two vacancy holes in neighboring layers as

$$E_f = \gamma\ (\pi d_1) + \gamma\ (\pi d_2), \qquad (1)$$

where γ is linear density of the edge formation energy of the vacancy hole and πd_1 and πd_2 are the circumferences of two vacancy holes. Denoting the diameters of one hole as d1, then the diameter of another hole can be written as

$$d_2 = \sqrt{[4A_T/\pi - d_1^2]}, \qquad (2)$$

where $A_T = \frac{1}{4}\pi(d_1^2 + d_2^2)$ is the total area of the two holes, which is a constant because of the mass reservation. So, the total formation energy of the two holes in different layers can be written as:

$$E_f = \gamma\ \{\pi d_1 + \pi \sqrt{[4A_T/\pi - d_1^2]}\} \qquad (3)$$

The maxim $E_f = \gamma \times \sqrt{(8\pi A_T)}$ appears at $d_1 = d_2 = \sqrt{(2 \times A_T/\pi\ )}$ and the minimum $E_f = \gamma \times \sqrt{(4\pi A_T)}$ appears at either d_1 or d_2 equals 0. This analysis clearly indicates that the two holes in different layers tend to become a big one by the interlayer migration of C atoms or vacancies. The atomic migration from a big one to a small one is energetically more preferable than that the reverse process because the total energy goes towards the global minimum in such a process. With such a driving force, facilitated with both intra- and inter- layer vacancy migrations, all the vacancies generated in MLG can be eventually gathered into a single hole in one layer, as observed in many experiments.[22, 37-39]

To achieve a deep insight into the driving force of interlayer vacancy migration, the relative formation energies of a serious of structures during the coalescence of two vacancy holes are shown in Fig. 4 In the initial configuration, a 6-fold and a 8-fold vacancy holes (V6 and V8) were created in top and bottom layers, respectively. By continuously removing C atoms from the large hole on the bottom layer to the small one on the top layer, the formation energy drops 14.08 eV in total (from V6 + V8 to V0 + V14). The energy barriers experienced during the whole process are 0.17, 2.71, 0.22, 1.69, 3.31, 0.55, 1.31 eV, respectively (Fig. 4). All these barriers are greatly lower than that of the SV migration between NGLs and most of them are significantly lower than that of the coalescence of two SVs in NGLs. This clearly indicated that the inter-layer migration barrier of two graphene holes could be further reduced. And, as expected, the formation energy of one large hole and one small one is always smaller than that of two equal sized holes. So the driving force tends to lead the system to the final configuration which has one perfect graphene layer and one large hole in another layer.

On the end, let’s exam the interlayer vacancy migration in large area of graphene. A large BLG model with 944 Carbon atoms and 40 vacancies in each layer (Fig. 5) was built and the classical MD simulation based the Brenner potential [40, 41] was performed. At 2500K, very similar scenery as that seen in Fig. 1 is shown. Although both layers are highly defective with 40 SVs, after 40 ns MD simulation, most area of the top layer are with clear hexagonal lattice and only a few small vacancy holes can be seen (one V6, one V3 and one V2). This implies a net mass transfer of 29 carbon atoms from the bottom layer to the top layer (actually there are 56 atoms migrate upwards and 27 atoms migrate downwards). In contrast, the bottom layer became very defective. There is a very large vacancy hole (V34) formed and a few small holes (one V10, one V6…) around. Certainly, if the simulation time could be macroscopic long, we can expect a perfect graphene on the top layer and a large hole in the bottom layer.

Conclusions

In summary, we have investigated migration behavior of the

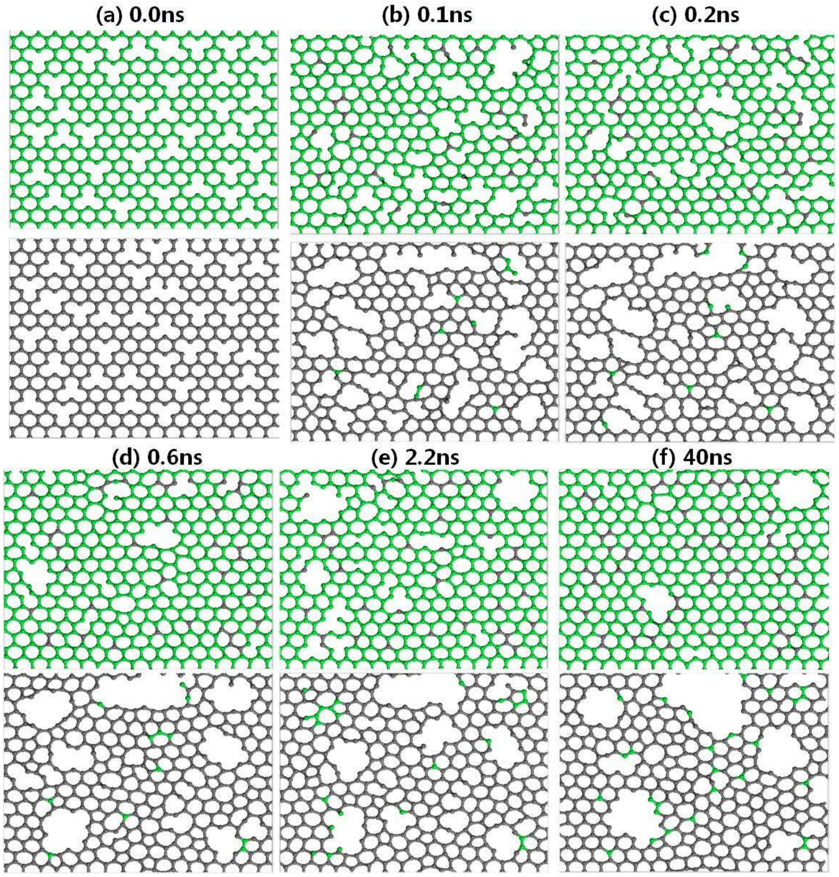

Fig. 5 The defect migration snapshots in graphene explored by molecular dynamic simulations (MD) with Brenner potential at 2500 K. The model have 80 vacancies totally in the beginning (each layer with 40 vacancies).

vacancies in single and multi-layer graphene (SLG/MLG) systematically with the QM/MD, classical MD simulations and the first principles calculations. It was found that in the single layer, vacancy defects prefer to coalesce into a larger vacancy holes. While, in the MLG, the vacancies tend to concentrate into one hole in one layer through both the intra- and inter- layer migrations. The vacancy interlayer migration is facilitated by the interaction of defects in neighboring layers. This study theoretically explains the puzzled experimental observation of vacancy interlayer migration and reveals a new mechanism of graphene healing. This deep insight into the mechanism of defect interlayer migration may leads to the technology of engineering of graphitic nanomaterials by electron/iron irradiation. conclusions section should come at the end of article.

Acknowledgements

The work of Hong Kong PolyU was supported by Hong Kong GRF research grant (G-YX4Q) and NSFC grant (21273189).

Notes and references

[a] *Beijing Computational Science Research Center, Beijing 100084, Peoples Republic of China*
[b] *A Institute of Textiles and Clothing, Hong Kong Polytechnic University, Kowloon, Hong Kong, Peoples Republic of China. feng.ding@polyu.edu.hk*
[c] *Institute of New Energy Material Chemistry, College of Chemistry, Nankai University, P. O. Box 300071, Tianjin, China*

†Electronic Supplementary Information (ESI) available: Optimized geometries and their total energies used in Fig. 3 and Fig. 4. See DOI: 10.1039/b000000x/

1 K. Mu□llen, J. P. Rabe, *Acc. Chem. Res.* 2008, **41**, 511-520.
2 S. R. Park, S. Ruoff, *Nat. Nanotechnol.* 2009, **4**, 217-224.
3 L. Britnell, R. Gorbachev, R. Jalil, B. Belle, F. Schedin, A. Mishchenko, T. Georgiou, M. Katsnelson, L. Eaves, S. Morozov, N. Peres, J. Leist, A. Geim, *Science.* 2012, **335**, 947-950.
4 J. Coraux, A. T. NDiaye, C. Busse, T. Michely, *Nano Lett.* 2008, **8**, 565-570.
5 O. Frank, M. Bousa, I. Riaz, R. Jalil, K. Novoselov, G. Tsoukleri, J. Parthenios, L. Kavan, K. Papagelis, C. Galiotis, *Nano Lett.* 2012, **12**, 687-693.
6 D. W. Boukhvalov, M. I. Katsnelson, *Nano Lett.* 2008, **8**, 4373-4379.
7 A. Lherbier, S. M. M. Dubois, X. Declerck, S. Roche, Y. Niquet, J. Charlier, *Phys. Rev. Lett.* 2011, **106**, 046803.
8 C. D. Latham, M. I. Heggie, J. A. Gμmez, I. Suμrez-Martínez, C. P. Ewels, P. R. Bridon, *J. Phys. Condens. Matter.* 2008, **20**, 395220.
9 R. Zan, Q. M. Ramasse, U. Bangert, K. S. Novoselov, *Nano Lett.* 2012, **12**, 3936-3940.
10 G. D. Lee, C. Z. Wang, E. N. Yoon, M. Hwang, D. Y. Kim, K. M. Ho, *Phys. Rev. Lett.* 2005, **95**, 205501.
11 A. Santana, A. M. Popov, E. Bichoutskaia, *Chem. Phys. Lett.* 2013, ***557,*** 80-87.
12 S. Kurasch, J. Kotakoski, O. Lehtinen, V. Skákalová, J. Smet, C. E. Krill, A. V. Krasheninnikov, U. Kaiser, *Nano Lett.* 2012, **12**, 3168-3173.

13 Q. Yuan, Xu, Z.; B. I. Yakobson, F.Ding, *Phys. Rev. Lett.* 2012, **108**, 245505.

14 X. Gao, L. Liu, S. Irle, S. Nagase, *Angew. Chem. Int. Ed.* 2010, **49**, 3200-3202.

15 F. Banhart, J. Kotakoski, A. V. Krasheninnikov, *ACS Nano.* 2011, 5, 26-41.

16 A. V. Krasheninnikov, K. Nordlund, M. Sirvio, E. Salonen, J. Keinonen, *Phys. Rev. B* 2001, **63**, 245405.

17 G. D. Lee, C. Z. Wang, E. Yoon, N. M. Hwang, K. M. Ho, *Phys. Rev. B* 2006, **74**, 245411.

18 M. H. Gass, U. Bangert, A. L. Bleloch, P. Wang, R. R. Nair, A. K. Geim, *Nat. Nanotechnol.* 2008, **3**, 676-681.

19 A. Hashimoto, K. Suenaga, A. Gloter, K. Urita, S. Iijima, *Nature* 2004, **430**, 870-873.

20 H. Zhang, M. Zhao, Xi. Yang, H. Xia, X. Liu, Y. Xia, *Diamond & Related Materials* 2010, **19**, 1240-1244.

21 M. T. Lusk, L. D. Carr, *Phys. Rev. Lett.* 2008, **100**, 175503.

22 J. Y. Huang, F. Ding, B. I. Yakobson, *Phys. Rev. B* 2008, **78**, 155436.

23 C. Jin, K. Suenaga, S. Iijima, *Nano Lett.* 2008, **8**, 1127-1130.

24 B. Aradi, B. Hourahine, T. Frauenheim, *J. Phys. Chem. A* 2007, **111**, 5678-5684.

25 http://www.dftb.org.

26 D. Porezag, T. Frauenheim, T. Köhler, G. Seifert, R. Kaschner, *Phys. Rev. B* 1995, **51**, 12947-12957.

27 G. Seifert, D. Porezag, T. Frauenheim, *Int. J. Quantum Chem.* 1996, **58**, 185-192.

28 G. Kresse, J. Furthmuller, *Phys. Rev. B* 1996, **54**, 11169.

29 G. Kresse, J. Furthmuller, *Comput. Mater. Sci.* 1996, **6**, 15-50.

30 J. P. Perdew, K. Burke, M. Ernzerhof, *Phys. Rev. Lett.* 1996, **77**, 3865.

31 P. E. Blöchl, *Phys. Rev. B* 1994, **50**, 17953-17979.

32 G. Henkelman, B. P. Uberuaga, H. Jónsson, *J. Chem. Phys.* 2000, **113**, 9901-9904.

33 R. Telling, C. Ewels, A. EL-Barbary, M. Heggle, *Nat. Mater.* 2003, **2**, 333-337.

34 L. Wang, X. Zhang, HL. Chan, F. Yan, F. Ding, *J. Am. Chem. Soc.* 2013, **135**, 4476-4482.

35 R.G. Amorim, A. Fazzio, A. Antonelli, F. D. Novaes, A.J. R. da Silva, *Nano Lett.* 2007, **7**, 2459-2462.

36 M. T. Lusk, L.D. Carr, *Phys. Rev. Lett.* 2008, **100**, 175503.

37 N. Lu, J. Wang, H. C. Floresca, M. J. Kim, *Carbon* 2012, **50**, 2961-2965.

38 J. Kotakoski, A.V. Krasheninnikov, U. Kaiser, J. C. Meyer, *Phys. Rev. Lett.* 2011, **106**, 105505.

39 W. Lin, K-S. Moon, S. Zhang, Y. Ding, J. Shang, M. Chen, C. Wong, *ACS Nano*, 2010, **4**, 1716-1722.

40 D. W. Brenner, *Phys. Rev. B* 1990, **42**, 9458-9471.

41 D. W. Brenner, O. A.Shenderova, J. A. Harrison, S. J. Stuart, B. Ni, S. B. Sinnott, *J. Phys.: Condens. Matter* 2002, **14**, 783-802.